

## IX.4 Hydrogen Safety Sensors

Eric L. Brosha<sup>1</sup>,  
Fernando H. Garzon<sup>1</sup> (Primary Contact),  
Robert S. Glass<sup>2</sup> (Primary Contact),  
Rangachary Mukundan<sup>1</sup>, Catherine G. Padro<sup>1</sup>,  
Praveen K. Sekhar<sup>1</sup>, and Leta Woo<sup>2</sup>

<sup>1</sup>Los Alamos National Laboratory  
MS D429, P.O. Box 1663  
Los Alamos, NM 87545  
Phone: (505) 667 6643  
E-mail: garzon@lanl.gov

<sup>2</sup>Lawrence Livermore National Laboratory  
L-103, P.O. Box 808, 7000 East Avenue  
Livermore, CA 94550  
Phone: (925) 423 7140  
E-mail: glass3@llnl.gov

DOE Technology Development Manager:  
Antonio Ruiz

Phone: (202) 586-0729  
E-mail: Antonio.Ruiz@ee.doe.gov

Project Start Date: 2008  
Project End Date: 2012

### Objectives

- Develop a low-cost, low-power, durable, and reliable hydrogen safety sensor for vehicle and infrastructure applications.
- Demonstrate working technology through application of commercial and reproducible manufacturing methods and rigorous life testing results guided by materials selection, sensor design, and electrochemical research and development investigation.
- Recommend sensor technologies and instrumentation approaches for engineering design.
- Disseminate packaged prototypes to DOE laboratories and commercial parties interested in testing and fielding advanced commercial prototypes while transferring technology to industry.

### Multi-Year Program Plan Technical Barriers from the Hydrogen Safety section (3.8) of the Fuel Cell Technologies Program

- (D) Liability Issues: Potential liability issues and lack of insurability affecting the commercialization of hydrogen technologies: Need for reliable H<sub>2</sub> safety sensor.

- (E) Variation in Standard Practice of Safety Assessments for Components and Energy Systems: the requirement to calibrate and commercialize safety sensors.
- (G) Expense of Data Collection and Maintenance

### Technical Targets

- Sensitivity: 1 vol% in air.
- Accuracy: 0.04-4% ± 1%.
- Response Time: <1 min at 1% and <1 sec at 4%; recovery <1 min.
- Temperature: -40°C to 60°C.
- Durability: 5 years without calibration.
- Cross-Sensitivity: Minimal interference to humidity, H<sub>2</sub>S, CH<sub>4</sub>, CO, and volatile organic compounds.

### Accomplishments

- New zirconia-based mixed potential sensor with 0-4 vol% hydrogen sensitivity was demonstrated utilizing a machined, dense indium-tin oxide (ITO) working electrode (In<sub>2</sub>O<sub>3</sub>; SnO<sub>2</sub>; 90%: 10%), a Pt wire counter electrode, and porous yttria-stabilized zirconia (YSZ) electrolyte were prepared using ceramic tape casting methods. The response of these devices to hydrogen concentrations up to 2% in air was studied from 600 to 740°C.
- Durability testing of over 1,700 hrs was accomplished on pre-commercial tape-cast sensors.
- Potential manufacturing platform were investigated for early prototypes.
- Developed a miniaturized, low-power, robust H<sub>2</sub> sensor prototype conducive to commercialization.
- Stable response over time achieved in the sensor prototype by modifying Pt morphology.
- Completed long-term testing of H<sub>2</sub> sensor (4,000 hrs) including 100 hrs of accelerated stress testing.
- Evaluated sensor electrode materials and design to further improve long-term stability and prevent sensor-aging effects.
- Investigated the suitability of lanthanum strontium manganate (LSM) as a pseudoconuter electrode to replace Pt electrode for long-term stability and reliability.
- Explored alternate modalities such as impedancemetric detection for H<sub>2</sub> screening.



## Introduction

Recent developments in the search for renewable energy coupled with the advancements in fuel cell powered vehicles have augmented the demand for hydrogen safety sensors [1]. There are several sensor technologies that have been developed to detect hydrogen, including deployed systems to detect leaks in manned space systems and hydrogen safety sensors for laboratory and industrial usage. Among the several sensing methods electrochemical devices [2-8] that utilize high temperature-based ceramic electrolytes are largely unaffected by changes in humidity and are more resilient to electrode or electrolyte poisoning. The desired sensing technique should meet a detection threshold of 1% (10,000 ppm) H<sub>2</sub> and response time of ≤1 sec [9] targets for infrastructure and vehicular. Further, a review of electrochemical hydrogen sensors by Korotcenkov et al [10] and the report by Glass et al [11] suggest the need for inexpensive, low-power, and compact sensors with long-term stability, minimal cross-sensitivity, and fast response. As part of the Hydrogen Codes and Standards sub-program, Los Alamos National Laboratory (LANL) and Lawrence Livermore National Laboratory (LLNL) are working together to develop and test inexpensive, zirconia-based, electrochemical (mixed potential) sensors for H<sub>2</sub> detection in air. Previous work conducted at LLNL showed [8] that ITO electrodes produced a stable mixed potential response in the presence of up to 5 % of H<sub>2</sub> in air with no response to CO<sub>2</sub> or water vapor. The sensor also showed desirable characteristics with respect to response time and resistance to aging, and degradation due to thermal cycling.

In this investigation, the development and testing of an electrochemical H<sub>2</sub> sensor prototype based on ITO/YSZ/Pt configuration is detailed. The device fabricated on an alumina substrate integrates a resistive Pt heater to achieve precise control of operating temperature while minimizing heterogeneous catalysis. Targeting fuel cell-powered automotive applications, the safety sensor was subjected to interference studies, temperature cycling, operating temperature variations, and long-term testing over 4,000 hrs. The sensor responded in real time to varying concentrations of H<sub>2</sub> (1,000 to 20,000 ppm). Among the interference gases tested such as NO, NO<sub>2</sub>, NH<sub>3</sub>, CO, and propylene (C<sub>3</sub>H<sub>6</sub>), the sensor showed cross-sensitivity to C<sub>3</sub>H<sub>6</sub>. Analyzing the overall device performance over 4,000 hrs of testing for 5,000 ppm of H<sub>2</sub>, (a) the sensitivity varied between 0.135 to 0.17 V with a minimum low of 0.12 V, (b) the baseline signal ranged from 0 to 0.04 V, and (c) the response rise time fluctuated between 3 to 47 s.

The salient features of the H<sub>2</sub> sensor prototype developed by LANL are (a) the low power consumption, (b) compactness to fit into critical areas of application, (c) simple operation, (d) fast response, (e) a direct

voltage read-out circumventing the need for any additional conditioning circuitry, and (f) conducive to commercialization.

## Approach

The sensor design approaches from LANL and LLNL were used to develop devices with superior performance.

### LANL Design: Controlled Electrode/Electrolyte/Gas Interface

At LANL, electrochemical potentiometric modality is utilized for designing the sensors. Mixed potential sensors are a class of electrochemical devices that develop an open-circuit electromotive force due to the difference in the kinetics of the redox reactions of various gaseous species at each electrode/electrolyte/gas interface, referred to as the triple phase boundary [12]. Therefore these sensors have been considered for the sensing of various reducible or oxidizable gas species in the presence of oxygen. Based on this principle, a unique sensor design was developed. The uniqueness of the LANL sensor [13] derives from minimizing heterogeneous catalysis (detrimental to sensor response) by avoiding gas diffusion through a catalytically active material and minimizing diffusion path to the 3-phase interface (electrode/electrolyte/gas referred to as triple phase boundary). Unlike the conventional design of these devices that use a dense solid electrolyte and porous thin film electrodes (similar to the current state-of-the-art zirconia-based sensors and fuel cells), the LANL design uses dense (either metal wires, oxide pellets or thin film) electrodes and porous electrolytes (bulk or thin film). Such a sensor design facilitates a stable and reproducible device response, since dense electrode morphologies are easy to reproduce and are significantly more stable than the conventional porous morphologies. Moreover, these sensors develop higher mixed potentials since the gas diffusion is through the less catalytically active electrolyte than the electrode. Further, the choice of electrodes is primarily based on their O<sub>2</sub> reduction kinetics. Sensors fabricated at LANL will typically involve one electrode with fast (Pt) and another with slow (Au or LaCrO<sub>3</sub>) O<sub>2</sub> reduction kinetics aimed to improve the sensitivity.

### LLNL Design

In the LLNL design, a new impedance-based measurement technique, originally developed for electrochemical NO<sub>x</sub> sensors, was shown to generate more stable sensor responses and may be able to offer a way to compensate for cross-sensitivity effects. The technique is based on the measurement of parameters related to the complex impedance of the sensor in the frequency range of 1 Hz to 10 kHz. Measurements

are typically made at a single frequency selected to maximize the desired sensitivity, although measurements performed at additional frequencies have been shown to be useful for correcting the response to interfering gases. LLNL has also found in the  $\text{NO}_x$  sensor studies that it may be possible to use a wider variety of electrodes for the sensor in impedance-based sensing. Additional possible advantages included better tolerance to mechanical defects (such as delamination) and better longer-term stability.

## Results

### (a) Potentiometric Sensing

Figure 1 shows the schematic of the fabricated sensor with integrated Pt heater. The plan and cross-sectional view of the sensor schematic along with the four post (two electrodes, two heater pads) metal connections are shown in the top and bottom part of Figure 1, respectively. After obtaining the sensor platform from ESL Electro-Science Laboratories (fabricated using a patented LANL design), the ITO electrode was deposited.

The ITO working electrode was sputter deposited onto the sensor body using a commercially available 2" diameter radio frequency magnetron sputtering target (Alfa,  $\text{In}_2\text{O}_3$ :  $\text{SnO}_2$ ; 90%: 10%) in an off-axis orientation. After ITO deposition, the YSZ electrolyte layer was prepared using e-beam evaporation. Tosoh-8z YSZ powder was pressed into a pellet, which was then sintered at  $1,200^\circ\text{C}$  for 6 hrs. The sintered pellet was used as the evaporation source. An alumina platform with four metal posts connecting the sensor electrodes and heater was housed in a low volume quartz tube with a gas inlet and outlet. Humidity was added to the system by passing the gas through a bubbler. The heater voltage was set to 6.5 V, which corresponded to an operating temperature of approximately  $535^\circ\text{C}$  following a polynomial trend,  $Y = 4.941x^2 + 45.85x + 28.16$  (Y represents the operating temperature in degrees and x represents the heater voltage).

The ITO and Pt electrode achieve different steady-state redox potentials when exposed to a mixture of  $\text{H}_2$  and  $\text{O}_2$  determined by the kinetic balance of the following electrochemical reactions:



The electrode that favors the second reaction over the first develops a large non-Nernstian potential. However, the non-electrochemical oxidation (heterogeneous catalysis) of  $\text{H}_2$  lowers the differential voltage developed between the electrodes signifying the importance of materials selection and localized heating.

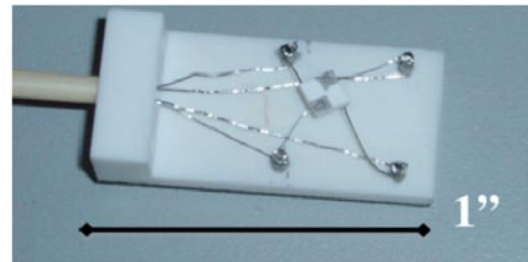
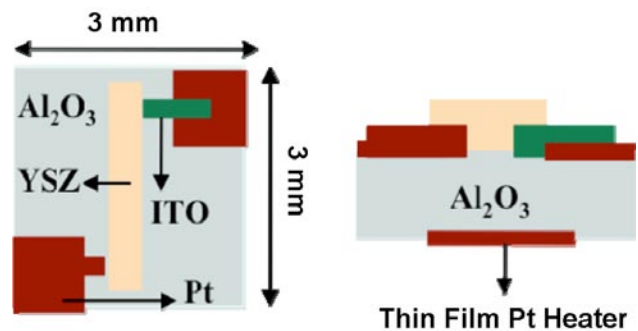


**FIGURE 1.** Schematic of the  $\text{H}_2$  Sensor Prototype with Integrated Pt Heater (Top) Plan and Cross-Sectional View of the Device and (Bottom) Four Post Metal Connection from the Device Sitting on an Alumina Platform

In this investigation, the alumina substrate is integrated with a screen-printed Pt heater for precise control over the operating temperature. In addition, the use of metal oxide electrode enables a higher mixed potential. The derived the mixed potential equation for a  $\text{H}_2$  sensor as a function of air/hydrogen concentration as:

$$E_M = E_0 + m \ln C_{\text{O}_2} - n \ln C_{\text{H}_2} \quad (\text{iii})$$

$E_M$  is the developed mixed potential,  $E_0$  is the electrode potential at equilibrium, m and n are constants, A is a constant associated with the catalytic activity of the electrode material through their dependence on the charge-transfer coefficient and the standard rate constant, and C stands for the concentration of  $\text{H}_2$  or  $\text{O}_2$ . As inferred from equation (iii), the mixed potential linearly relates with logarithmic concentrations of  $\text{H}_2$ . Such an observation is noticed in this investigation.

Figure 2a shows the staircase sensor response with varying concentrations of  $\text{H}_2$ . The sensor response was seen to linearly vary with logarithmic concentrations of  $\text{H}_2$  and seems to follow a mixed potential device behavior.

For interference studies, 100 ppm of gases such as NO,  $\text{NO}_2$ , CO,  $\text{NH}_3$  and  $\text{C}_3\text{H}_6$  were used as analytes. Figure 2b shows the cross-sensitivity response indicating a strong signal from 100 ppm of  $\text{C}_3\text{H}_6$ . The concentration of  $\text{C}_3\text{H}_6$  was further increased to 500 ppm to observe any augment in the undesired signal. Absence of any

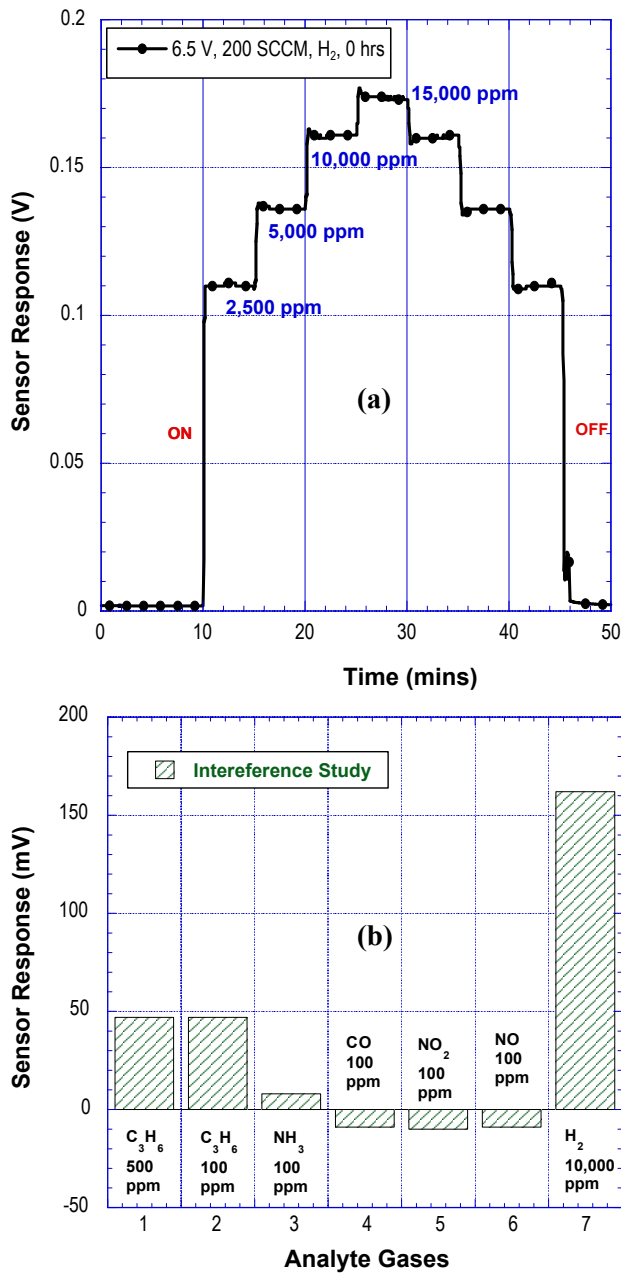


**FIGURE 2.** (a) Sensor response upon exposure to various concentrations of H<sub>2</sub> in air (6.5 V~535°C, 200 SCCM, 0 hrs) and (b) Cross-sensitivity studies comparing sensor response from 10,000 ppm of H<sub>2</sub> to 100 ppm of interferents and 500 ppm of C<sub>3</sub>H<sub>6</sub>.

significant increase in the C<sub>3</sub>H<sub>6</sub> response with higher concentration suggests that the tested concentration range of C<sub>3</sub>H<sub>6</sub> must have coincided with the saturation region of the device (characterized by the logarithmic flat sensor response). Also, the occurrence of a non-electrochemical heterogeneous process rather than electrochemical oxidation of C<sub>3</sub>H<sub>6</sub> cannot be ruled out.

Life cycle characterization of the sensor was initiated since the device exhibited the appropriate

**TABLE 1.** Summary of the Life Cycle Testing Experiments

Time (hrs)	Conditions
0 - 300	Set Voltage – 6.5 V, Maintaining Humidity Level and Base Gas
301 - 390	Temperature Cycling 6.5 V to 0 to 6.5 V, Three Cycles, Maintaining Humidity Level and Base Gas
391 - 822	Set Voltage – 6.5 V, Maintaining Humidity Level and Base Gas
823 - 894	Operating Temperature Variations – 6.5 to 5.75 V, Maintaining Humidity Level and Base Gas
895 - 1900	Static Conditions – No humidity, No Base Gas, Set Voltage – 6.5 V
1901 - 2296	Set Voltage – 6.5 V, Maintaining Humidity Level and Base Gas
2297 - 3249	Set Voltage – 6.5 V, Maintaining Humidity Level and Base Gas
3250 - 4000	Stress Testing – Temperature Cycling 6.5 V to 0: 100, 500, 1000, and 10000 Cycles, Sensor Response Measurement Before and After Each Cycle

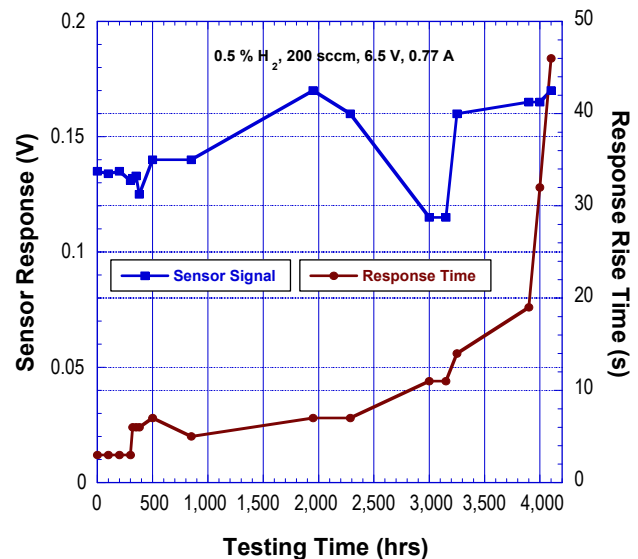


**FIGURE 3.** Lifetime testing of sensor response and response time upon exposure to 5,000 ppm of H<sub>2</sub> over 4,000 hrs (6.5 V~535°C, 200 SCCM, air)

sensitivity and selectivity to H<sub>2</sub>. Table 1 summarizes the different sensor testing conditions over 4,000 hrs. The variation in the sensor response (Figure 3) subjected to different thermal treatments can be attributed to thermal expansion mismatch between the electrodes (ITO, Pt) and the electrolyte (YSZ). For a typical ceramic-metal system involving high-temperature applications, the recommended rule for materials selection involves the



use of metal, that have similar and/or smaller thermal expansion coefficients than that of the ceramic. Though intermediate layers (such as an insulator or metal composites) have been added in the past to match the coefficient of thermal expansion (CTE) of the metal and the ceramic, certain applications that involve charge transfer process demand a direct ceramic-metal contact. Considering the materials specific to this application, the thermal expansion coefficients of ITO, 8z-YSZ, and Pt from published literature were found to be  $6.2 \times 10^{-6}/^{\circ}\text{C}$ ,  $9.6 \times 10^{-6}/^{\circ}\text{C}$ , and  $10.53 \times 10^{-6}/^{\circ}\text{C}$  respectively. The CTE of both ITO and Pt electrode deviate from that of YSZ. Such a variation in CTE of the materials may be responsible for the different levels of sensor response observed in Figure 3. The variation in the sensor response subjected to different thermal treatments is also shown in Figure 3. As the response time of the device is governed by the speed of the competing oxygen reduction and electrochemical oxidation reactions, it is postulated that surface stress on ITO due to CTE mismatch and  $\text{H}_2$  oxidation slows down the reaction represented in equation (ii) upon different thermal treatments.

Analyzing the overall device performance from 0 to 4,000 hrs upon exposure to 5,000 ppm of  $\text{H}_2$ , (a) the sensitivity varied between 0.135 to 0.17 V with a minimum low of 0.12 V, (b) the baseline signal ranged from 0 to 0.04 V, and (c) the response rise time fluctuated between 3 to 47 s. It should be noted that the rise time includes the time constant of the test set-up, which is calculated as 1 s. The absence of any dramatic deterioration in the sensor response over time is attributed to a stable three-phase interface (electrode/electrolyte/gas). As the interfacial regions contain the electrochemically active sites, it is vulnerable to microstructural changes during sensor operation as these regions are also the sites for mass transport and diffusion. These microstructural changes (for example, due to annealing/heating) can be a major factor inducing sensor drift. Even well designed interfaces contribute to the electrical losses of devices and hence limit the overall sensor performance. Hence, it is critical to engineer the interface through materials selection and processing for the development of a reliable and stable sensor

### (b) Impedancemetric Sensing

Based on preliminary results, impedance-based response was evaluated using a test cell with a stacked electrode configuration consisting of a porous ITO sensing electrode on the bottom, porous YSZ electrolyte, and dense LSM counter electrode on the top. Results of impedance-based testing indicated reasonably stable performance to over 150 hrs of testing with resolution of 0.25, 0.5, 1, and 2 vol%  $\text{H}_2$ . However, the sensitivity for the impedance-based method was lower than that of the

potentiometric signal. Nevertheless, another important result of the impedance-based sensing experiments was characterizing the overall influence of applied signals (alternating and direct current, ac and dc) on the stability of the sensor response during long-term testing. Further investigation is necessary to understand how applied signals may temporarily influence sensing behavior, and the development of a novel strategy using electrical measurement and conditioning protocols, both alternating current and direct current, will be explored to improve sensor performance.

## Conclusions

- Improved electrode materials with potentially better performance were investigated where dense electronically conducting oxide (LSM) counter electrode showed better long-term stability.
- An alternate impedancemetric sensing modality was explored to evaluate improvements in long-term performance and stability.
- A pre-commercial  $\text{H}_2$  sensor prototype was fabricated on an alumina substrate with ITO and Pt electrodes and YSZ electrolyte with an integrated Pt heater to achieve precise operating temperature and minimize heterogeneous catalysis.
- During the initial 4,000 hrs of long-term testing for the prototype with optimized platinum electrode, the sensor response to 5,000 ppm of  $\text{H}_2$  varied at a maximum of ca. +10%/-7% from its original value of 0.135 V (0 hrs). The response rise time fluctuated between 3 to 47 s.
- The extended sensor response stability over time may be attributed to a stable, engineered three-phase interface.
- The salient features of the investigated  $\text{H}_2$  sensor prototype include (a) conducive to commercialization, (b) low power consumption, (c) compactness to fit into critical areas, (d) simple transduction mechanism, and (e) fast response.

## Future Directions

- Postmortem analysis of  $\text{H}_2$  prototype sensor tested for 4,000 hrs (Aug. 2010 - Oct. 2010).
- Fabrication and lifetime performance evaluation (minimum 5,000 hours) of advanced prototypes (Aug. 2010 - Feb. 2011).
  - Investigation of composite electrode compositions with novel impregnation technique for improved stability. Such a rationale is based on controlling properties at the interface between the electrode and electrolyte. The composite electrode compositions, containing both electrode and electrolyte material may decrease

thermal expansion mismatch at the interface and improve stability. Further, the novel impregnation technique uses an already sintered backbone of electrolyte material where the electrode material is added in a separate low-temperature process step (previous work has shown this approach to not only improve thermal expansion matching (as anticipated with a composite structure), but also improve electronic/ionic conduction paths).

- Cross-sensitivity studies, stability evaluation using LSM electrodes in advanced prototypes (Sep. 2010 - Dec. 2010).
  - Need to configure radio frequency magnetron sputter system and optimize deposition conditions for lanthanum strontium manganese oxide (LSMO) thin film deposition. This material will replace Pt as a sensor pseudo-reference counter electrode. Then, sputter masks (for low- and high-temperature depositions) needs to be prepared for sensor electrode and electrolyte film patterning during deposition. Also, a modified mount needs to be machined to fix position of sensor substrate relative to mask. This will permit a high degree of reproducibility for placement of electrodes/ electrolyte from sensor to sensor. Finally, several ITO and LSMO calibration runs needs to be performed to characterize rates/structure/morphology/conductivity.
- Characterize and understand the sensing mechanism(s) in various modalities and apply to future devices and optimize next generation of pre-commercial prototypes (Sept. 2010).
- Investigate and identify packaging schemes for field and laboratory testing (Nov. 2010 - Jan. 2011).
- Independent testing and comparison of the performance of packaged prototype H<sub>2</sub> sensor with a commercial device (Feb. 2011 - May 2011).
  - Initiate and pursue collaboration and independent testing work with Dr. William Buttner from National Renewable Energy Laboratory. Then, acquisition of best available technology H<sub>2</sub> sensor (thermal conductivity detector-based technology, \$2000.00 unit cost) for comparison performance/stability testing with the low-cost LANL/LLNL device needs to be completed.
  - Further, a new, customized test chamber assembly needs to be constructed to test H<sub>2</sub> sensors (both experimental and commercial) under diffusion conditions while permitting continuous sampling and measurement of [H<sub>2</sub>] local to sensors using gas chromatography.

## FY 2010 Patent Application

1. B.S.Farber, J.Kaniuk, R.Proch, **P.K.Sekhar**, E.L.Brosha, R.Mukundan, and F.H.Garzon, “Sensor and method for reliable detection of high concentrations of Hydrogen and avoiding cross-interference with other gases”, Submitted to LANL Patent Office, 2010.

## FY 2010 Publications and Presentation

1. P.K.Sekhar, E.L.Brosha, R. Mukundan, T. L. Williamson, M.A.Nelson and F.H.Garzon, “**Development and Testing of a Hydrogen Safety Sensor Prototype**”, Sensors and Actuators B, 148, 469 (2010).
2. E.L.Brosha, P.K.Sekhar, R.Mukundan, T.L.Williamson, F.H.Garzon, L.Y.Woo, and R.S.Glass, “**Development of Sensors and Sensing Technology for Hydrogen Fuel Cell Vehicle Applications**”, ECS Transactions, 26 (1), 475 (2010).
3. P.K.Sekhar, E.L.Brosha, R. Mukundan, and F.H.Garzon, “**Development of a Reliable, Miniaturized Hydrogen Safety Sensor Prototype**”, Fuel Cell Seminar and Exposition, Oct 18-22, 2010.
4. L.Y.Woo, R.S.Glass, P.K.Sekhar, E.L.Brosha, R.Mukundan, M.A.Nelson and F.H.Garzon, “**Electrode Stability in Hydrogen Sensors Based on Yttria-Stabilized Zirconia Electrolyte**”, 217<sup>th</sup> ECS Meeting in Vancouver, BC, Canada, April 2010.
5. P.K.Sekhar, E.L.Brosha, R.Mukundan, M.A.Nelson and F.H.Garzon, “**Electrical Characterization of a Mixed Potential Sensor based on Indium Tin Oxide and Lanthanum Strontium Chromite Electrodes and Yttria-Stabilized Zirconia Electrolyte**”, 34<sup>th</sup> International Conference and Exposition on Advanced Ceramics and Composites, Jan 24-29, 2010.
6. E.L.Brosha, P.K.Sekhar, R.Mukundan, T.L.Williamson, F.H.Garzon, L.Y.Woo, and R.S.Glass, “**Development of Sensors and Sensing technology for Hydrogen Fuel Cell Vehicle Applications**”, 2009 Fuel Cell Seminar, Palm Springs, CA.

## References

1. L. Boon-Brett, J. Bousek, G. Black, P. Moretto, P. Castello, T. Hübert, and U. Banach, Identifying performance gaps in hydrogen safety sensor technology for automotive and stationary applications, International Journal of Hydrogen Energy, 35 (2010), 373-384.
2. H.Iwahara, H.Uchida, K.Ogaki and H.Nagato, Nernstian Hydrogen Sensor Using BaCeO<sub>3</sub>-Based, Proton-Conducting Ceramics Operative at 200-900°C, Journal of The Electrochemical Society, 138 (1991), 295-299.
3. Y.Tan and T.C. Tan, Characteristics and Modeling of a Solid State Hydrogen Sensor, The Journal of Electrochemical Society, 141 (1994), 461-466.

4. Z.Samec, F.Opekar, and G.J.E.F. Crijns, Solid-state Hydrogen Sensor Based on a Solid-Polymer Electrolyte, *Electroanalysis*, 7 (1995), 1054-1058.
5. Y-C.Liu, B-J. Hwang, and I.J.Tzeng, Solid-State Amperometric Hydrogen Sensor Using Pt/C/Nafion Composite Electrodes Prepared by a Hot-Pressed Method, *Journal of The Electrochemical Society*, 149 (2002), H173-H178.
6. L.B. Kriksunov, and D.D. Macdonald, Amperometric hydrogen sensor for high-temperature water, *Sensors and Actuators B*, 32 (1996), 57-60.
7. G.Lu, N.Miura, and N.Yamazoe, High-temperature hydrogen sensor based on stabilized zirconia and a metal oxide electrode, *Sensors and Actuators B*, 35-36 (1996), 130-135.
8. L.P. Martin and R.S. Glass, Hydrogen Sensor Based on Ytria-Stabilized Zirconia Electrolyte and Tin-Doped Indium Oxide Electrode, *Journal of The Electrochemical Society*, 152 (2005), H43-H47.
9. R.S. Glass, J. Milliken, K. Howden, R. Sullivan (Eds.), *Sensor Needs and Requirements for Proton-Exchange Membrane Fuel Cell Systems and Direct-Injection Engines*, 2000, pp. 7 – 15. DOE, UCRL-ID-137767.
10. G.Korotcenkov, S.D.Han and J.R.Stetter, Review of Electrochemical Hydrogen Sensors, *Chemical Review*, 109 (2009), 1402-1433.
11. L.P. Martin and R.S. Glass, Electrochemical Sensors for PEMFC Vehicles, presented at The 2004 DOE Hydrogen, Fuel Cells, and Infrastructure Technologies Program Review, Philadelphia, PA (May 27, 2004).
12. F.H.Garzon, R.Mukundan, and E.L.Broscha, Solid state mixed potential gas sensors: theory, experiments and challenges, *Solid State Ionics*, 136-137 (2000), 633-638.
13. P.K.Sekhar, E.L.Broscha, R.Mukundan, M.A.Nelson and F.H.Garzon, Application of Commercial Automotive Sensor Manufacturing Methods for NO<sub>x</sub>/NH<sub>3</sub> Mixed Potential Sensors for Emission Control, *ECS Transactions*. 19 (2009), 45-49.